Eur. Phys. J. C 7, 487–499 (1999)
DOI 10.1007/s100529801011

THE EUROPEAN
PHYSICAL JOURNAL C

The rare K-decays in the Multiscale Walking Technicolor Model

Z.J. Xiao[1,2,a], L.X. Lü[2], H.K. Guo[2], G.R. Lu[1,2]

[1] CCAST(World Laboratory) P.O. Box 8730, Beijing 100080, P.R. China
[2] Department of Physics, Henan Normal University, Xinxiang, 453002 P.R. China[b]

Received: 17 June 1998 / Revised version: 12 August 1998 / Published online: 6 November 1998

Abstract. We calculate the one-loop Z^0-penguin contributions to the rare K-decays, $K^+ \to \pi^+\nu\bar{\nu}$, $K_L \to \pi^0\nu\bar{\nu}$ and $K_L \to \mu^+\mu^-$, from the unit-charged technipions π_1 and π_8 in the framework of the Multiscale Walking Technicolor Model. We find that: (a) the π_1 and π_8 can provide one to two orders enhancements to the branching ratios of the rare K-decays; (b) by comparing the experimental data of $Br(K^+ \to \pi^+\nu\bar{\nu})$ with the theoretical prediction one finds the lower mass bounds, $m_{p8} \geq 249\,\mathrm{GeV}$ for $F_Q = 40\,\mathrm{GeV}$ and $m_{p1} = 100\,\mathrm{GeV}$; (c) by comparing the experimental data of $Br(K_L \to \mu^+\mu^-)$ with the theoretical predictions one finds the lower bounds on m_{p1} and m_{p8}, $m_{p1} \geq 210\,\mathrm{GeV}$ if only the contribution from π_1 is taken into account, and $m_{p8} \geq 580\,\mathrm{GeV}$ for $m_{p1} = 210\,\mathrm{GeV}$, assuming $F_Q = 40\,\mathrm{GeV}$; (d) the assumed ranges of the masses m_{p1} and m_{p8} in the Multiscale Walking Technicolor Model are excluded by the rare K-decay data.

1 Introduction

In the framework of the Standard Model(SM), the rare K-decays $K^+ \to \pi^+\nu\overline{\nu}$, $K_L \to \pi^0\nu\overline{\nu}$ and $K_L \to \mu^+\mu^-$ are all loop-induced semileptonic flavour-changing neutral current(FCNC) processes determined by Z^0-penguin and W-box diagrams. These decay modes have very similar structure, and depend on one or two basic functions out of the set ($X(x_t)$, $P_0(X)$, $Y(x_t)$, and $P_0(Y)$) [1,2]. The decay $K^+ \to \pi^+\nu\bar{\nu}$ is CP conserving and receives contributions from both internal top and charm quark exchanges, while the decay $K_L \to \pi^0\nu\bar{\nu}$ proceeds almost entirely through direct CP violation and is completely determined by short-distance loop diagrams with top quark exchanges. For the decay $K_L \to \mu^+\mu^-$, the short-distance part can also be calculated reliably.

The rare K-decay processes are very good place to probe the effects of new physics beyond the SM because these rare decay modes are very clean theoretically. Firstly, the short-distance contributions to the rare K-decays can be calculated reliably and the long-distance parts to the first two decays $K^+ \to \pi^+\nu\overline{\nu}$ and $K_L \to \pi^0\nu\overline{\nu}$ are negligibly small. For the decay $K_L \to \mu^+\mu^-$, the long-distance contributions from the two-photon intermediate state which are large and difficult to be calculated reliably [3] because of its unperturbitive nature, but we here only consider the new physics effects on the short-distance contributions to the rare K-decay modes. Secondly, the inclusion of next-to-leading order (NLO) QCD corrections reduces considerably the theoretical uncertainty due to the choice of the renormalization scales μ_t and μ_c. Thirdly, the discovery of top quark and the measurement of its mass reduce significantly another major source of theoretical uncertainty. These clean semileptonic decays are also very well suited for the determination of CKM matrix elements V_{ts}, V_{td} as well as the Wolfenstein parameters ρ and η, but we do not study such topics in this paper.

As is well-known, Technicolor (TC) [4] is one of the important candidates for the mechanism of naturally breaking electroweak symmetry. To generate ordinary fermion masses, extended technicolor (ETC) [5] models have been proposed. The original ETC models suffer from two serious problems: predicting too large flavor changing neutral currents (FCNC's) and too small masses for the second and third generation fermions. In walking technicolor theories[6], the first large FCNC problem can be resolved and the fermion masses can be increased significantly by the large enhancement due to the walking effects of α_{TC}[6]. The often-discussed QCD-like one generation technicolor model(OGTM) [7] predicted a rather large oblique correction parameter S [8]: $S \approx 1.6$ for $N_{TC} = 4$, which is contradict with the fitted value of $S = -0.16 \pm 0.14$ [9]. But we know that these estimates do not apply to models of walking technicolor because the integrals of weak-current spectral functions and their moments converge much more slowly than they do in QCD and consequently simple dominance of spectral integrals by a few resonances cannot be correct [10]. According to the estimations done in [11], the S parameter can be small or even negative in the walking technicolor models[11]. To explain the large hierarchy of the quark masses, multiscale walking technicolor models (MWTCM) are further constructed[12]. The MWTCM also predicted a large number of technirhos and technipions which are shown to be testable in experiments[10, 13]. So it is interesting to study the possible contribu-

[a] e-mail: dphnu@public.zz.ha.cn
[b] Mailing address

tions to the rare K-decays from the unit-charged color-singlet and color-octet technipions in the framework of the MWTCM[12].

In the "Penguin Box expansion" (PBE) approach[14], the decay amplitude for a given decay mode can be written as

$$A(decay) = P_0(decay) + \sum_r P_r(decay)\, F_r(x_t) \qquad (1)$$

where the $F_r(x_t)$ are the basic, universal, process independent but m_t-dependent functions [1] with corresponding coefficients P_r characteristic for the decay under consideration; and the m_t-independent term P_0 summarizes contributions stemming from internal quarks other than the top, in particular the charm quark.

In a previous paper[15], we calculated the Z^0-penguin and box contributions from the unit-charged technipions to the rare K-decays in the framework of the one generation technicolor model[7]. In this paper, we will estimate the corresponding contributions to the rare K-decays in the framework of MWTCM[12]. Our strategy for the current work is rather simple: we evaluate the Z^0-penguin and box diagrams induced by the charged technipions, compare the relevant analytical expressions of effective couplings with the corresponding expressions in the SM, separate the new functions C_0^{New} and C_{NL}^{New}, which summarize the effects of the new physics beyond the SM, and finally combine the new functions with their counterparts in the SM and use the new basic functions directly in the calculation for specific decays.

From the numerical calculations, we find that the unit-charged color-singlet and color-octet technipions π_1 and π_8 appeared in the MWTCM can provide two to three orders enhancement to the branching ratios of the rare K-decays. The contribution from the color-singlet π_1 is positive but relatively small in size, and therefore the color-octet technipion π_8 dominates the total contributions.

By comparing the experimental data of the rare K-decays with the theoretical predictions one can obtain the lower bounds on the masses of charged technipions[2]. For the decay mode $K^+ \to \pi^+\nu\overline{\nu}$, the lower mass bounds are $m_{p8} \geq 249,228\,\text{GeV}$ for $F_Q = 40\,\text{GeV}$ and $m_{p1} = 100,200\,\text{GeV}$ respectively; For the decay mode $K_L \to \mu^+\mu^-$, the lower mass bound on m_{p1} is $m_{p1} \geq 210\,\text{GeV}$ if only the contribution from π_1 is taken into account and assuming $F_Q = 40\,\text{GeV}$, while the lower mass bound on m_{p8} is $m_{p8} \geq 580\,\text{GeV}$ assuming $F_Q = 40\,\text{GeV}$ and $m_{p1} = 210\,\text{GeV}$. For $F_Q = 30\,\text{GeV}$, the above lower mass bounds will be increased by about 50 GeV. For $F_Q = 40\,\text{GeV}$ and $m_{p8} = 490\,\text{GeV}$ the whole parameter space for m_{p1} is excluded completely. For the decay mode $K_L \to \pi^0\nu\overline{\nu}$, however, no lower mass bounds could be derived because of the low sensitivity of the corresponding experimental data. The assumed ranges of the masses m_{p1} and m_{p8} in the Multiscale Walking Technicolor Model[12] are excluded by the rare K-decay data, and therefore the specific model[12] itself is disfavored by the data.

This paper is organized as follows. In Sect. 2 we describe the basic structures of the MWTCM, briefly review the properties of the charged technipions π_1 and π_8, and present the effective Z^0-penguin couplings with the inclusion of technipion contributions. In the following three sections, we calculate the new contributions to the decays $K^+ \to \pi^+\nu\overline{\nu}$, $K_L \to \pi^0\nu\overline{\nu}$ and $K_L \to \mu^+\mu^-$ respectively and try to extract the possible lower mass bounds on charged technipions by comparing the theoretical predictions with the corresponding experimental data. The conclusions and discussions are included in the final section.

2 Effective $d\bar{s}Z$ coupling and relevant formulae

The rare FCNC K- and B-decays have been investigated at the NLO level within the framework of the SM. Consequently, the relevant formulae and the systematic analysis in the SM can be found easily in new review papers [1, 2]. The impact of some scenarios of new physics on the rare K- and B-decays has been considered for instance in [15–19]. In this paper we will investigate the contributions to the rare FCNC K-decays from the unit-charged technipions π_1 and π_8 in the framework of the MWTCM.

2.1 Basic structures of the MWTCM

In [12], the authors constructed a specific multiscale walking technicolor model and investigated its phenomenology. The major features of this model relevant with our studies are the following:

1. This model contains one doublet $\psi = (\psi_U, \psi_D)$ of color-singlet technifermions in the antisymmetric tensor representation A_2 of $SU(N_{TC})$; one doublet of color-triplet techniquarks, $Q = (U, D)$; and N_L doublets of color-singlet technileptons, $L_m = (N_m, E_m)$, $m = 1, \cdots, N_L$. Under the gauge group $SU(N_{TC}) \otimes SU(3) \otimes SU(N_L) \otimes SU(2)_I$[3] the technifermions are

$$\begin{aligned} T_{3L,R} &\equiv \psi_{L,R} \in (A_2, 1, 1, 2), \\ T_{2L,R} &\equiv Q_{L,R} \in (N_{TC}, 3, 1, 2), \\ T_{1L,R} &\equiv L_{L,R} \in (N_{TC}, 1, N_L, 2). \end{aligned} \qquad (2)$$

2. They assumed that the technifermion chiral-symmetry breaking scales Λ_i, the condensates $< \bar{T}_i T_i >$, the π_T decay constant F_i $(i = L, Q, \pi)$ may be estimated

[1] The complete set of functions $F_r(x_t)$ include: $S_0(x_t)$, $X_0(x_t)$, $Y_0(x_t)$, $Z_0(x_t)$, $E_0(x_t)$, $D_0^{'}(x_t)$ and $E_0^{'}(x_t)$, as given explicitly in [1]

[2] In [12], the authors used the symbol $\pi_{\bar{D}U}$ and $\pi_{D\bar{U}}$ to denote the unit-charged color-octet technipions, we here use the symbol π_8. We also use the π_1 to denote the physical mixed state of the P_1^+ and P_2^+, and use the m_{p1} and m_{p8} to denote the masses of π_1 and π_8

[3] Which is obtained by two steps of breaking from the ETC gauge group $SU(N_{ETC})_1 \otimes SU(N_{ETC})_2$ as described in [12]

from the corresponding QCD parameters by naive scaling and large N_{TC} arguments. They studied the phenomenology under the limits of $\Lambda_\pi >> \Lambda_Q \cong \Lambda_L$ and $F_\psi >> F_Q \cong F_L$ with the constraint

$$\sqrt{N_L F_L^2 + 3F_Q^2 + F_\psi^2} = v = 246\,\mathrm{GeV} \tag{3}$$

where $F_Q = 20 \sim 40\,\mathrm{GeV}$.

3. This model predicted a rich spectrum of technipions. Among them are unit-charged color-octets $\pi^a_{\bar{D}U}$ and $\pi^a_{\bar{U}D}$, and unit-charged color-singlets P_1^+ and P_2^+, which will contribute to the rare K-decays in question through the Z^0-penguin and box diagrams.
4. The authors calculated the dijet and technipion production rates at $\bar{p}p$ colliders by using two sets of input parameters. The Set-A and Set-B mass parameters (all masses are in GEV) are:

$$\begin{aligned} Set-A:\ & F_L = 28,\ F_Q = 29,\ M_{P_1^+} = 172, \\ & M_{P_2^+} = 251,\ M_{\pi_{\bar{D}U}} = 261, \cdots, \end{aligned} \tag{4}$$

and

$$\begin{aligned} Set-B:\ & F_L = 41,\ F_Q = 43,\ M_{P_1^+} = 218, \\ & M_{P_2^+} = 311,\ M_{\pi_{\bar{D}U}} = 318, \cdots, \end{aligned} \tag{5}$$

The technipion $\pi^a_{\bar{D}U}$ in [12] is just the same technipion as the P_8^+ appeared in the one-generation technicolor model[7,20], and the technipions P_1^+ and P_2^+ are mainly $\bar{E}N$ and $\bar{D}U$ with small $\overline{\psi_D}\psi_U$ piece and therefore the mixed state π_1 of the P_1^+ and P_2^+ is the same kind of technipion as P^+ given in [7,20]. We will study the new contributions to the rare K-decays from the physical mixed state π_1 instead of the two technipions P_1^+ and P_2^+, for the sake of simplicity.

If these technipions are relatively light as assumed in [12] they will contribute to various production and decay processes effectively. At the Tevatron and LHC, they can be pair produced copiously, as discussed systematically in [10,12,13,21,22]. In this paper, we calculate the new contributions to the rare K-decays from the π_1 and π_8 as described in the MWTCM [12]. For the rare K-decays under consideration, the charged technipions may contribute through the $d\bar{s}Z$-penguin and box diagrams by effective technipion-fermion pair and Z^0-technipion pair Yukawa couplings.

The color-singlet technipion π_1 is the closest analog to the charged Higgs boson $H^\pm$ in the two Higgs doublet model[23], but the color-octet technipion is rather different with the $H^\pm$ since it carries color and therefore is involved in the QCD and ETC strong interaction as well as the electroweak interactions. It is this fact which makes the difference between the charged Higgs bosons and unit-charged technipions.

The most model-independent limit on the mass of $H^\pm$[24], $M(H^\pm) \geq 44\,\mathrm{GeV}$, also apply to π_1. The color-octet technipion π_8 receives QCD, electroweak and extended technicolor (ETC) contributions to its mass, one previous estimation predicted that $M(\pi_8) \approx 200\,\mathrm{GeV}$[20]. In walking technicolor, however, the large ratio $< \bar{T}T >_{ETC} / < \bar{T}T >_{TC}$ will enhance technipion masses, and consequently the technipions in walking technicolor models are generally heavier than those in the ordinary OGTM. Unfortunately, it is almost impossible to predict the masses of technipions reliably at present. What one can do is a qualitative estimation about the range of those masses, as has been done in [12], where the authors estimated the contributions to technipion masses from different sources and gave the typical ranges: $M(P^+) = 170 \sim 320\,\mathrm{GeV}$ and $M(\pi_{\bar{D}U}) = 250 \sim 320\,\mathrm{GeV}$ corresponding their choice for different sets of parameters. In this paper, we treat the masses of π_1 and π_8 as semi-free parameters, varying in the ranges of $50\,\mathrm{GeV} \leq m_{p1} \leq 400\,\mathrm{GeV}$ and $100\,\mathrm{GeV} \leq m_{p8} \leq 600\,\mathrm{GeV}$ respectively. Generally speaking, the color-singlet π_1 should be lighter than the color-octet π_8.

The ETC interaction couples technifermions to quarks and leptons, and so governs the couplings between technipions and fermion pairs. Such effective Yukawa couplings are therefore ETC model dependent. According to the conventional wisdom, which is inspired by analogy with the SM, the technipions couple essentially to fermion masses. In other words, these effective Yukawa couplings are Higgs-like, and so the couplings between technipions and heavy fermions (especially the third generation fermions) will be dominant. According to the estimations done by J. Ellis et al. [20,26], the effective Yukawa couplings of charged technipions to fermion pairs can be written as [20,26],

$$\begin{aligned} &(\frac{-i}{F_\pi})\,\pi_1^+ \left\{ V_{KM}\,(m_d\,\overline{u_L}\,d_R - m_u\,\overline{u_R}\,d_L)\,\sqrt{2/3} \right. \\ &\left. -\sqrt{6} m_e\,\overline{\nu_{eL}}\,e_R \right\} + h.c., \end{aligned} \tag{6}$$

$$\begin{aligned} &(\frac{-i}{F_\pi})\,\pi_{8\alpha}^+ \left\{ V_{KM}\,(m_d \overline{u_L}\,\lambda^\alpha\,d_R - m_u \overline{u_R}\,\lambda^\alpha\,d_L) \right\}\,2 \\ &+h.c., \end{aligned} \tag{7}$$

where the $L, R = (1 \mp \gamma_5)/2$, the u and d stand for the up and down type quarks (u, c, t) and (d, s, b) respectively, the e denotes the leptons (e, μ, τ), the λ^α $(\alpha = 1, \cdots, 8)$ are the Gell-Mann $SU(3)_C$ matrices, the V_{KM} is the element of CKM matrix. The technipion decay constant F_π is model dependent: $F_\pi = 123\,\mathrm{GeV}$ in the often-discussed OGTM, while $F_\pi = F_Q = 20 \sim 40\,\mathrm{GeV}$ in the multiscale walking technicolor model[12] in order to produce the correct masses for the gauge bosons Z^0 and W.

The gauge interactions of technipions with the standard model gauge bosons occur dynamically through technifermion loops. At low energy scales well below the Technicolor scale their couplings to gauge bosons can be evaluated reliably by using well-known techniques of current algebra or effective lagrangian methods [12,20,25]. The relevant gauge couplings of Z^0 gauge boson to charged technipion pairs can be written as [20,27],

$$Z\pi_1^+\pi_1^- : \quad -ig\frac{1 - 2\sin^2\theta_W}{2\cos\theta_W}(p^+ - p^-)\cdot\epsilon \tag{8}$$

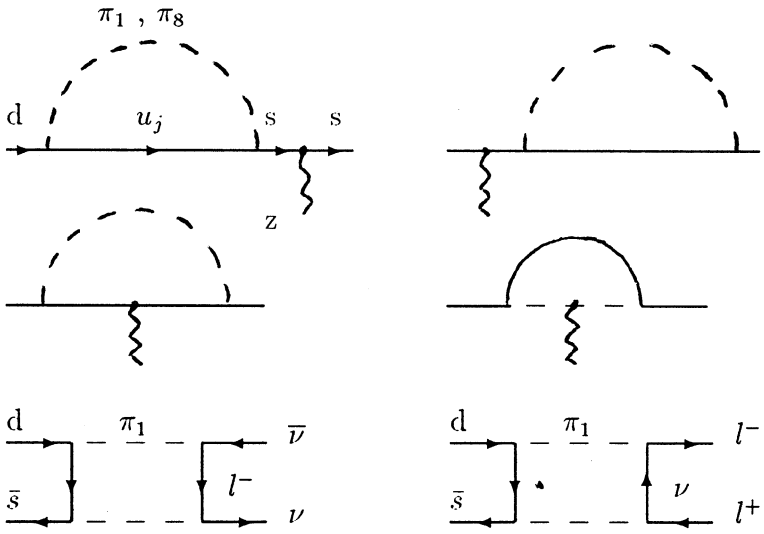

Fig. 1. The new Z^0-penguin diagrams contributing to the induced $d\bar{s}Z$ vertex from the internal exchanges of the technipion π_1 and π_8. The dashed lines are π_1 and π_8 lines and the u_j stands for the quarks (u, c, t)

Fig. 2. The new box diagrams contributing to the studied processes by internal exchanges of color-singlet π_1

$$Z\pi^+_{8\alpha}\pi^-_{8\beta}: \quad -ig\frac{1-2\sin^2\theta_W}{2\cos\theta_W}(p^+-p^-)\cdot\epsilon\,\delta_{\alpha\beta} \qquad (9)$$

where the $\sin\theta_W$ is the Weinberg angle, the p^+ and p^- are technipion momenta and the ϵ is the polarization vector of Z^0 gauge boson.

2.2 The Z^0-penguin and box diagrams

The new one-loop diagrams for the induced $d\bar{s}Z$ couplings due to the exchange of the technipions π_1 and π_8 are shown in Fig. 1. Figure 2 shows the box diagrams when the W gauge boson internal lines are replaced by color-singlet technipion lines. The color-octet π_8 does not couple to the $l\nu$ lepton pairs, and therefore does not present in the box diagrams. The corresponding one-loop diagrams in the SM were evaluated long time ago and can be found in [28]. We here just draw the new one-loop diagrams where the technipion propergators are inserted in all possible ways under the t' Hooft-Feynman gauge.

Because of the lightness of the s and d quarks when compared with the large top quark mass and the technipion masses we set $m_s = 0$ and $m_d = 0$ in the calculation. We will use dimensional regularization to regulate all the ultraviolet divergences in the virtual loop corrections and adopt the $\overline{MS}$ renormalization scheme. It is easy to show that all ultraviolet divergences are canceled for π_1 and π_8 respectively, and therefore the total sum is also finite.

By analytical evaluations of the Feynman diagrams as shown in Fig. 1, we find the effective $d\bar{s}Z$ vertex induced by the π_1 exchanges,

$$\Gamma^I_{Z_\mu} = \frac{1}{16\pi^2}\frac{g^3}{\cos\theta_W}\sum_j \lambda_j\,\overline{s_L}\,\gamma_\mu\,d_L\;C_0^{New}(y_j) \qquad (10)$$

with

$$C_0^{New}(y_j) = \eta^a_{TC}\left[\frac{y_j(-1+2\sin^2\theta_W-3y_j+2\sin^2\theta_W y_j)}{8(1-y_j)} - \frac{\cos^2\theta_W y_j^2}{2(1-y_j)^2}\ln[y_j]\right] \qquad (11)$$

and

$$\eta^a_{TC} = \frac{m^2_{p1}}{24\sqrt{2}F_Q^2 G_F M_W^2}\,, \qquad (12)$$

where $\lambda_j = V^*_{js}V_{jd}$, $y_j = m_j^2/m_{p1}^2$, and the $G_F = 1.16639(2)\times10^{-5}(\,\mathrm{GeV}^{-2})$ is the Fermi coupling constant.

For the case of color-octet π_8, the effective $d\bar{s}Z$ vertex induced by the π_8 exchanges is the form of,

$$\Gamma^{II}_{Z_\mu} = \frac{1}{16\pi^2}\frac{g^3}{\cos\theta_W}\sum_j \lambda_j\,\overline{s_L}\,\gamma_\mu\,d_L\;C_0^{New}(z_j) \qquad (13)$$

with

$$C_0^{New}(z_j) = \eta^b_{TC}\left[\frac{z_j(-1+2\sin^2\theta_W-3z_j+2\sin^2\theta_W z_j)}{8(1-z_j)} - \frac{\cos^2\theta_W z_j^2}{2(1-z_j)^2}\ln[z_j]\right] \qquad (14)$$

and

$$\eta^b_{TC} = \frac{m^2_{p8}}{3\sqrt{2}F_Q^2 G_F M_W^2} \qquad (15)$$

where $z_j = m_j^2/m_{p8}^2$.

When compared with (2.6) of [28], one can see that the $C_0^{New}(y_j)$ and $C_0^{New}(z_j)$ in (11,14) are just the same kind of terms as the function Γ_Z in (2.7) of [28] or the basic function $C_0(x_i)$ in (2.18) of [1]. The $C_0^{New}(y_j)$ describes the contributions to the $d\bar{s}Z$ vertex from the color-singlet technipion π_1, while the $C_0^{New}(z_j)$ describes the contributions from the color-octet technipion π_8.

In the above calculations, we used the unitary relation $\sum_{j=u,c,t}\lambda_j\cdot\ constant = 0$ wherever possible, and

neglected all terms proportional to p^2, p'^2 and $p \cdot p'$ ($p' = p - k$). This is a conventional approximation. We also used the functions $(B_0, B_\mu, C_0, C_\mu, C_{\mu\nu})$ whenever needed to make the integrations, and the explicit forms of these complicated functions can be found, for instance, in the Appendix-A of [29].

For the color-singlet π_1, it does couple to $l\nu$ pairs through box diagram as shown in Fig. 2, but the relevant couplings are strongly suppressed by the lightness of m_l. Even for the τ lepton, the corresponding cross section still be suppressed by an additional factor of $m_\tau^2/F_Q^2 \sim 10^{-3}$. Consequently, we can neglect the tiny contributions from π_1 through the box diagrams safely. The color-octet π_8 does not couple to any lepton pairs, and therefore can not contribute to the rare K-decays through the Box diagrams. In short, the technipion π_1 and π_8 contribute effectively to the rare K-decays through the Z^0-penguin diagrams only. We therefore can include the contributions from π_1 and π_8 to the rare K-decays by simply adding the functions C_0^{New} with the function $C_0(x_i)$ given in [1].

2.3 Basic functions at the NLO level

Within the standard model, the decay $K^+ \to \pi^+\nu\overline{\nu}$ depends on the functions $X(x_t)$ and X_{NL}^l relevant for the top part and charm part respectively, and the decay $K_L \to \pi^0\nu\overline{\nu}$ depends on one basic function $X(x_t)$, while the short-distance part of the decay $K_L \to \mu^+\mu^-$ depends on the functions $Y(x_t)$ (the top part) and Y_{NL} (the charm part) [1,2],

$$X(x_t) = X_0(x_t) + \frac{\alpha_s}{4\pi} X_1(x_t), \tag{16}$$

$$Y(x_t) = Y_0(x_t) + \frac{\alpha_s}{4\pi} Y_1(x_t), \tag{17}$$

$$X_{NL}^l = C_{NL} - 4B_{NL}^{1/2}, \tag{18}$$

$$Y_{NL} = C_{NL} - B_{NL}^{-1/2} \tag{19}$$

where the functions $X_0(x_t)$ and $Y_0(x_t)$ are leading contributions

$$\begin{aligned} X_0(x_t) &= C_0(x_t) - 4B_0(x_t), \\ Y_0(x_t) &= C_0(x_t) - B_0(x_t) \end{aligned} \tag{20}$$

and the functions $X_1(x_t)$ and $Y_1(x_t)$ are QCD corrections, and finally the function C_{NL} is the Z^0-penguin part in the charm sector, the functions $B_{NL}^{1/2}$ and $B_{NL}^{-1/2}$ are the box contributions in the charm sector, relevant for the case of final state neutrinos (leptons) with weak isospin $T_3 = 1/2$ $(-1/2)$ respectively. In [1], the authors also defined the functions $P_0(X)$ and $P_0(Y)$ for the decay $K^+ \to \pi^+\nu\overline{\nu}$ and $K_L \to \mu^+\mu^-$ respectively,

$$P_0(X)^{SM} = \frac{1}{\lambda}\left[\frac{2}{3}X_{NL}^e + \frac{1}{3}X_{NL}^\tau\right], \tag{21}$$

$$P_0(Y)^{SM} = \frac{Y_{NL}}{\lambda^4}. \tag{22}$$

The P_0 functions describe the contributions from the charm sector.

When the new contributions from charged technipions are included, the functions X, Y and P_0 can be written as

$$X(x_t, y_t, z_t) = X(x_t) + C_0^{New}(y_t) + C_0^{New}(z_t), \tag{23}$$

$$Y(x_t, y_t, z_t) = Y(x_t) + C_0^{New}(y_t) + C_0^{New}(z_t), \tag{24}$$

$$P_0(X) = P_0(X)^{SM} + \frac{1}{\lambda}\left[C_{NL}(\pi_1) + C_{NL}(\pi_8)\right] \tag{25}$$

$$P_0(Y) = P_0(Y)^{SM} + \frac{1}{\lambda^4}\left[C_{NL}(\pi_1) + C_{NL}(\pi_8)\right] \tag{26}$$

Where the functions $C_0^{New}(y_t)$ and $C_0^{New}(z_t)$ are given in (11,14). For completeness, we present the expressions for the functions $C_0(x_t)$, $B_0(x_t)$, $X_1(x_t)$, $Y_1(x_t)$, C_{NL}, $B_{NL}^{1/2}$, $B_{NL}^{-1/2}$, $C_{NL}(\pi_1)$ and $C_{NL}(\pi_8)$ in the Appendix. One can also find the explicit expressions for the relevant functions within the Standard Model in [1,2].

In this paper we do not investigate the uncertainties in the prediction for the branching ratios of rare K-decays related to the choice of the renormalization scales μ_t and μ_c in the top part and the charm part, respectively. In the numerical calculations, we fix the relevant parameters as follows and use them as the Standard Input (all masses are in GeV):

$$\begin{aligned} &M_W = 80.2,\ G_F = 1.16639 \times 10^{-5}\,\mathrm{GeV}^{-2}, \\ &\alpha = 1/129,\ \sin^2\theta_W = 0.23,\ m_c \equiv \overline{m_c}(m_c) = 1.3, \\ &m_t \equiv \overline{m_t}(m_t) = 170,\ \mu_c = 1.3,\ \mu_t = 170, \\ &\Lambda_{\overline{MS}}^{(4)} = 0.325,\ \Lambda_{\overline{MS}}^{(5)} = 0.225,\ A = 0.84, \\ &\lambda = 0.22,\ \rho = 0,\ \eta = 0.36 \end{aligned} \tag{27}$$

where the A, λ, ρ and η are Wolfenstein parameters at the leading order. For $\alpha_s(\mu)$ we use the two-loop expression as given in [2],

$$\alpha_s(\mu) = \frac{4\pi}{\beta_0 \ln(\mu^2/\Lambda^2)}\left[1 - \frac{\beta_1}{\beta_0^2}\cdot\frac{\ln\ln(\mu^2/\Lambda^2)}{\ln(\mu^2/\Lambda^2)}\right], \tag{28}$$

with

$$\beta_0 = \frac{33 - 2N_f}{3}, \quad \beta_1 = 102 - 10N_f - 8N_f/3 \tag{29}$$

where the N_f is the number of quark flavours.

In the SM, using the input parameters as given in (27), one obtains $X(x_t) = 1.539$, $P_0(X)^{SM} = 0.352$, $Y(x_t) = 1.04$, and $P_0(Y)^{SM} = 0.150$. These values are in very good agreement with those given in [1].

When the contributions from the technipions are included, the X, Y and P functions generally depend on the masses of the π_1 and π_8. The color-octet π_8 dominate the total contribution because of the color enhancement.

Figure 3a shows the m_{p8} dependence of the $X(x_t)$ function assuming $F_Q = 40\,\mathrm{GeV}$. The short-dashed line is the contribution in the SM. The π_1 provide a positive contribution, the typical value is $X(x_t)(\pi_1) = 1.352$ for $m_{p1} = 100\,\mathrm{GeV}$. The π_8 can provide a rather large positive contribution to the function $X(x_t)$ when it is light, one typical

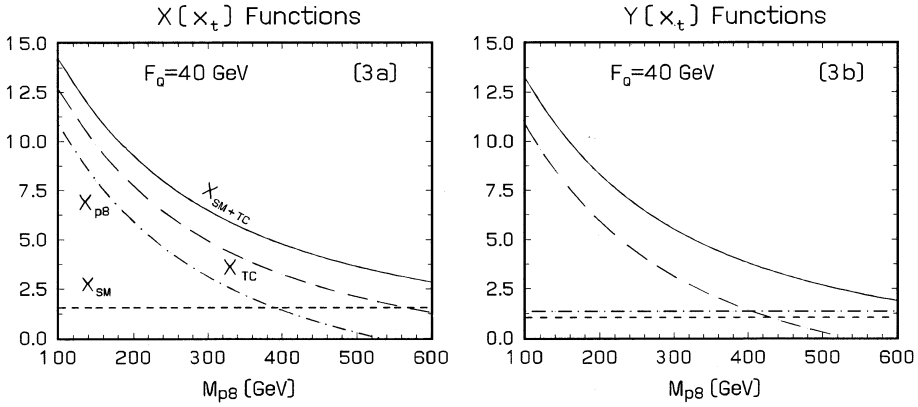

Fig. 3. a, **b** are the plots of the functions $X(x_t)$ and $Y(x_t)$ vs the mass m_{p8}. For more details see the text

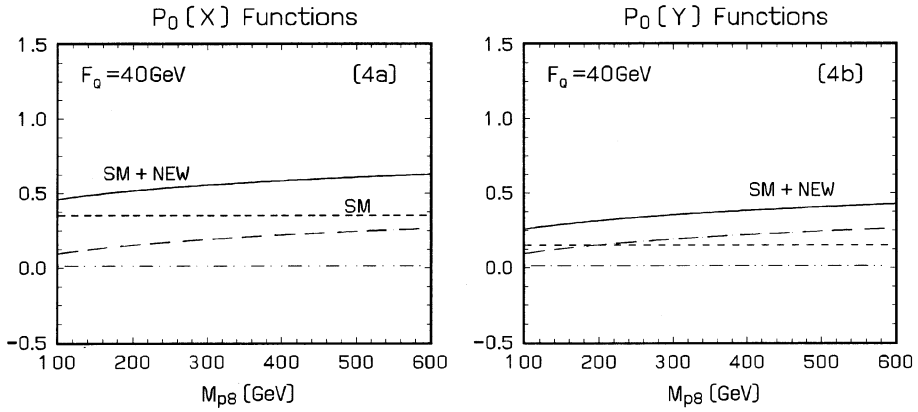

Fig. 4. a, **b** are the plots of the functions $P_0(X)$ and $P_0(Y)$ vs the mass m_{p8}. For more details see the text

value is $X(x_t)(\pi_8) = 3.127$ for $m_{p8} = 300\,\text{GeV}$. The contribution will become negative for $m_{p8} \geq 531\,\text{GeV}$. The long-dashed line shows the total contribution for both π_1 and π_8. The solid line represents the total contribution.

Figure 3b shows the m_{p8} dependence of the function $Y(x_t)$ assuming $F_Q = 40\,\text{GeV}$. The short-dashed line is the contribution in the SM. The charged technipions provide the same kinds of contributions to the function $Y(x_t)$ as that to $X(x_t)$. The dot-dashed line shows the contribution from the π_1 for $m_{p1} = 100\,\text{GeV}$. The long-dashed line shows the contribution from π_8 and the solid line represents the total contribution. For smaller F_Q, the size of the functions $X(x_t)$ and $Y(x_t)$ will become more larger.

Figure 4a and Fig. 4b are plots of functions $P_0(X)$ and $P_0(Y)$ vs m_{p8}. The short-dashed line shows the $P_0(X)$ and $P_0(Y)$ in the SM, the dot-dashed lines are the contributions from π_1 for $m_{p1} = 100\,\text{GeV}$. The typical values are $P_0(X)(\pi_1) = P_0(Y)(\pi_1) = 0.012$ for $m_{p1} = 100\,\text{GeV}$ and $P_0(X)(\pi_8) = P_0(Y)(\pi_8) = 0.152$ for $m_{p8} = 200\,\text{GeV}$. The solid line again shows the total contribution.

3 The decay $K^+ \to \pi^+\nu\overline{\nu}$

Within the Standard Model, the effective Hamiltonian for $K^+ \to \pi^+\nu\overline{\nu}$ are now available at the NLO level [1],

$$\mathcal{H}_{eff} = \frac{G_F}{\sqrt{2}}\frac{\alpha}{2\pi\sin^2\theta_W}\sum_{l=e,\mu,\tau}\left(V_{cs}^*V_{cd}X_{NL}^l + V_{ts}^*V_{td}X(x_t)\right) \times(\overline{s}d)_{V-A}(\overline{\nu_l}\nu_l)_{V-A} \tag{30}$$

where the functions $X(x_t)$ and X_{NL}^l have been given in (16,18).

Using the effective Hamiltonian (30) and summing over the three neutrino flavors one finds

$$Br(K^+ \to \pi^+\nu\overline{\nu}) = \kappa_+ \cdot \left[\left(\frac{Im\lambda_t}{\lambda^5}X(x_t)\right)^2 + \left(\frac{Re\lambda_c}{\lambda}P_0(X)^{SM} + \frac{Re\lambda_t}{\lambda^5}X(x_t)\right)^2\right] \tag{31}$$

where $\kappa_+ = 4.11 \times 10^{-11}$[1], and $\lambda = 0.22$ is the Wolfenstein parameter.

When the new contributions are included, one finds

$$Br(K^+ \to \pi^+\nu\overline{\nu}) = \kappa_+ \cdot \left[\left(\frac{Im\lambda_t}{\lambda^5}X(x_t,y_t,z_t)\right)^2 + \left(\frac{Re\lambda_c}{\lambda}P_0(X) + \frac{Re\lambda_t}{\lambda^5}X(x_t,y_t,z_t)\right)^2\right] \tag{32}$$

Within the SM, using the input parameters of (27), one finds

$$Br(K^+ \to \pi^+\nu\bar{\nu}) = 8.72 \times 10^{-11}, \tag{33}$$

which is consistent with the result given in [1]. When the contributions due to π_1 and π_8 are included, the size of the corresponding branching ratios depends on the masses m_{p1} and m_{p8}. Using the input parameters of (27) and

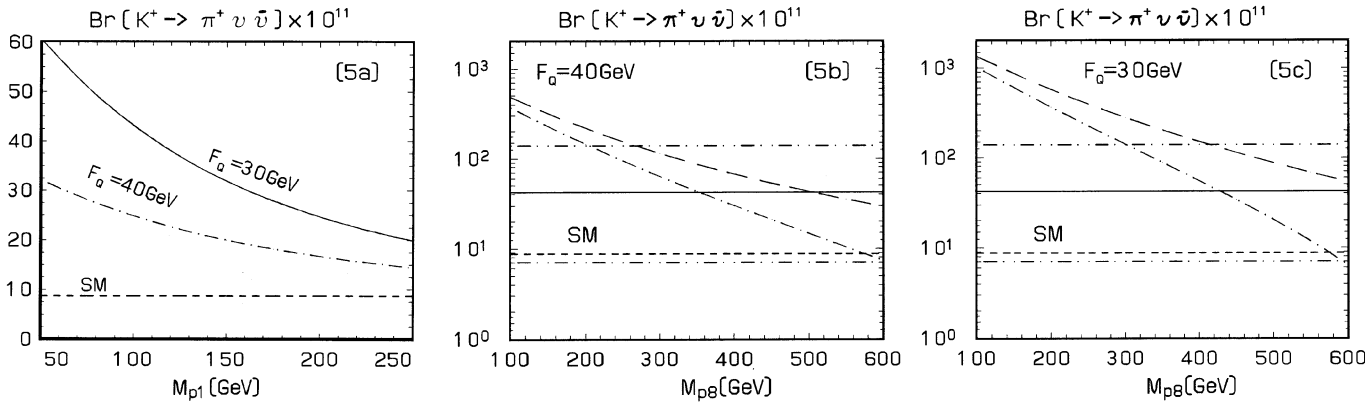

Fig. 5. **a** is the plot of the branching ratio $Br(K^+ \to \pi^+\nu\bar{\nu})$ vs the mass m_{p1} for $F_Q = 30, 40\,\text{GeV}$ respectively, **b**, **c** are the plots of the branching ratio $Br(K^+ \to \pi^+\nu\bar{\nu})$ vs the mass m_{p8} for $F_Q = 30, 40\,\text{GeV}$ respectively. For more details see the text

assuming $F_Q = 40\,\text{GeV}$, $50\,\text{GeV} \leq m_{p1} \leq 400\,\text{GeV}$ and $100\,\text{GeV} \leq m_{p8} \leq 600\,\text{GeV}$, one finds

$$1.07 \times 10^{-10} \leq Br(K^+ \to \pi^+\nu\bar{\nu}) \leq 3.21 \times 10^{-10} \quad (34)$$

if only the π_1's contribution is included, and

$$7.34 \times 10^{-11} \leq Br(K^+ \to \pi^+\nu\bar{\nu}) \leq 3.69 \times 10^{-9} \quad (35)$$

if only the π_8's contribution is included, and

$$9.14 \times 10^{-11} \leq Br(K^+ \to \pi^+\nu\bar{\nu}) \leq 4.81 \times 10^{-9} \quad (36)$$

if the π_1's and π_8's contribution are all included.

For the typical values of $F_Q = 40\,\text{GeV}$, $m_{p1} = 200\,\text{GeV}$ and $m_{p8} = 300\,\text{GeV}$, one has

$$Br(K^+ \to \pi^+\nu\bar{\nu}) = \begin{cases} 8.72 \times 10^{-11} \text{ in the SM} \\ 1.67 \times 10^{-10} \text{ only } \pi_1 \text{ considered} \\ 6.33 \times 10^{-10} \text{ only } \pi_8 \text{ considered} \\ 8.27 \times 10^{-10} \text{ both } \pi_1 \text{ and } \pi_8 \text{ considered.} \end{cases} \quad (37)$$

The new experimental bound on $Br(K^+ \to \pi^+\nu\bar{\nu})$ is[31]:

$$Br(K^+ \to \pi^+\nu\bar{\nu})_{exp} = 4.2^{+9.7}_{-3.5} \times 10^{-10} \quad (38)$$

which is close to the SM expectations (33), and begins to cross the range of the theoretical expectations when the new contributions from the charged technipions are included. There is no lower limit on m_{p1} if we neglect the contribution from the π_8. The lower mass bound on π_8 depends on the values of the F_Q and m_{p1}:

$$m_{p8} \geq 249,\ 228\,\text{GeV} \quad (39)$$

for $F_Q = 40\,\text{GeV}$ and $m_{p1} = 100, 200\,\text{GeV}$ respectively. For $F_Q = 30\,\text{GeV}$ and $m_{p1} = 200\,\text{GeV}$, one has $m_{p8} \geq 341\,\text{GeV}$.

Figure 5a shows the m_{p1} dependence of the branching ratios $Br(K^+ \to \pi^+\nu\bar{\nu})$ when only the contribution from π_1 is included. The short-dashed line corresponds to the Standard Model prediction, and the long-dashed line (solid line) shows the theoretical prediction for $F_Q = 40\,\text{GeV}$ ($30\,\text{GeV}$) respectively.

Figure 5b shows the m_{p8} dependence of the branching ratios $Br(K^+ \to \pi^+\nu\bar{\nu})$ when the contributions from both π_1 and π_8 are considered. The horizontal band corresponds to the experimental data (38). The short-dashed line shows the SM prediction, while the dot-dashed curve shows the branching ratio when only the new contribution from the π_8 is taken into account. The long-dashed curve shows the branching ratio when the new contributions from both π_1 and π_8 are included and assuming $m_{p1} = 50\,\text{GeV}$. Figure 5c also show the mass dependence of the branching ratios $Br(K^+ \to \pi^+\nu\bar{\nu})$ but for $F_Q = 30\,\text{GeV}$ and $m_{p1} = 50\,\text{GeV}$.

If we consider the theoretical uncertainty of the branching ratio $Br(K^+ \to \pi^+\nu\bar{\nu})$ in the SM, say about $\pm 4 \times 10^{-11}$[1], the above lower mass bounds will be decreased by no more than 4 GeV. It is easy to see that the the uncertainty of the experimental data is still rather large and dominate the total uncertainty. Consequently, further reduction of the experimental error is very essential to constrain the Multiscale Walking Technicolor Model more stringently.

4 The decay $K_L \to \pi^0\nu\bar{\nu}$

Since the rare decay $K_L \to \pi^0\nu\bar{\nu}$ proceeds in the SM almost entirely through CP violation [34], it is completely dominated by short-distance loop effects with the top quark exchanges. The charm contribution can be safely neglected and there is no theoretical uncertainties due to m_c, μ_c and $\Lambda_{\overline{MS}}$ present in the decay $K^+ \to \pi^+\nu\bar{\nu}$. At the level of $Br(K_L \to \pi^0\nu\bar{\nu})$ the uncertainty in the choice of μ_t is reduced from $\pm 10\%$ (LO) down to $\pm 1\%$ (NLO), and therefore can also be neglected[1]. Consequently this decay mode is even cleaner than $K^+ \to \pi^+\nu\bar{\nu}$ and is very well suited for the probe of new physics if the experimental data can reach the required sensitivity.

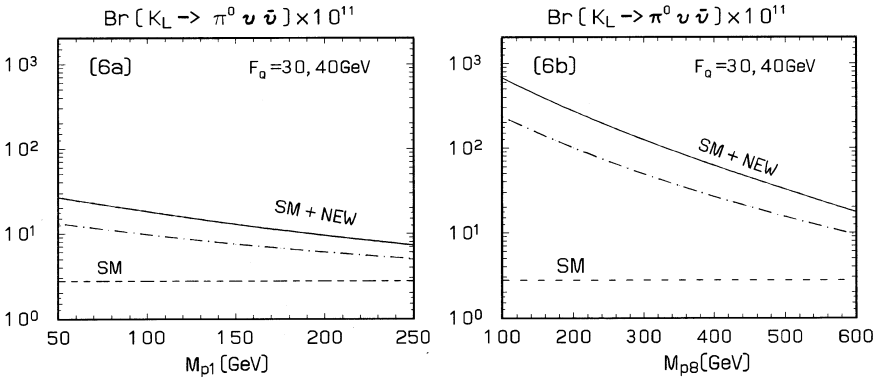

Fig. 6. a, **b** are the plots of the branching ratio $Br(K_L \to \pi^0\nu\bar{\nu})$ vs the mass m_{p1} and m_{p8} and assuming $F_Q = 30, 40\,\mathrm{GeV}$ respectively. For more details see the text

The effective Hamiltonian for $K_L \to \pi^0\nu\bar{\nu}$ is given as follows[1],

$$\mathcal{H}_{eff} = \frac{G_F}{\sqrt{2}}\frac{\alpha}{2\pi\sin^2\theta_W}V_{ts}^*V_{td}X(x_t)(\bar{s}d)_{V-A}(\bar{\nu}\nu)_{V-A} + h.c., \quad (40)$$

where the functions $X(x_t)$ has been given in (16).

Using the effective Hamiltonian (40) and summing over three neutrino flavors one finds

$$Br(K_L \to \pi^0\nu\bar{\nu}) = \kappa_L \cdot \left(\frac{Im\lambda_t}{\lambda^5}X(x_t)\right)^2 \quad (41)$$

with $\kappa_L = 1.80 \times 10^{-10}$[1].

In the Standard Model, using the input parameters of (27), one finds

$$Br(K_L \to \pi^0\nu\bar{\nu}) = 2.75 \times 10^{-11} \quad (42)$$

which is consistent with the result given in [1]. When the contributions due to π_1 and π_8 are included, the size of the corresponding branching ratios depends on the masses m_{p1} and m_{p8}. Using the input parameters of (27) and assuming $F_Q = 40\,\mathrm{GeV}$, $50\,\mathrm{GeV} \le m_{p1} \le 400\,\mathrm{GeV}$ and $100\,\mathrm{GeV} \le m_{p8} \le 600\,\mathrm{GeV}$, one finds

$$3.42 \times 10^{-11} \le Br(K_L \to \pi^0\nu\bar{\nu}) \le 1.31 \times 10^{-10} \quad (43)$$

if only the π_1's contribution is included, and

$$1.23 \times 10^{-11} \le Br(K_L \to \pi^0\nu\bar{\nu}) \le 1.77 \times 10^{-9} \quad (44)$$

if only the π_8's contribution is included, and

$$1.69 \times 10^{-10} \le Br(K_L \to \pi^0\nu\bar{\nu}) \le 2.33 \times 10^{-9} \quad (45)$$

if the π_1's and π_8's contributions are all included. For the typical values of $m_{p1} = 200\,\mathrm{GeV}$ and $m_{p8} = 300\,\mathrm{GeV}$, one has $Br(K_L \to \pi^0\nu\bar{\nu})(\pi_1) = 6.03 \times 10^{-11}$, $Br(K_L \to \pi^0\nu\bar{\nu})(\pi_8) = 2.53 \times 10^{-10}$ and $Br(K_L \to \pi^0\nu\bar{\nu})(All) = 3.39 \times 10^{-10}$.

Figure 6a shows the m_{p1} dependence of the branching ratio $Br(K_L \to \pi^0\nu\bar{\nu})$ when only the new contribution from π_1 is considered. The dot-dashed (solid) curve represents the theoretical prediction for $F_Q = 40$ (30) GeV respectively. Figure 6b shows the m_{p8} dependence of the branching ratio $Br(K_L \to \pi^0\nu\bar{\nu})$ when the contributions from both π_1 and π_8 are considered, assuming $m_{p1} = 50\,\mathrm{GeV}$. The dot-dashed (solid) curve again shows the theoretical prediction for $F_Q = 40$ (30) GeV respectively.

The present experimental bound on $Br(K_L \to \pi^0\nu\bar{\nu})$ from FNAL experiment E731 [35] is $Br(K_L \to \pi^0\nu\bar{\nu}) < 5.8 \times 10^{-5}$, which is about six orders of magnitude above the SM expectation and about four orders of magnitude above the theoretical prediction when the maximum new contributions from the charged technipions are included. There is obviously a long way to go for the forthcoming or planed experiments [33,36] to measure this gold-plated decay mode with enough sensitivity to probe the effects of new physics.

5 The decay $K_L \to \mu^+\mu^-$

For the decay $K_L \to \mu^+\mu^-$, the situation is more complicated because of the presence of long-distance contributions from the two-photon intermediated state which are difficult to calculate reliably [3]. But one important advantage is the availability of the experimental data with good sensitivity[9]. In this paper we only consider the new physics effects to the short distance part $(K_L \to \mu^+\mu^-)_{SD}$.

In the Standard Model, the effective Hamiltonian for $K_L \to \mu^+\mu^-$ are now available at the NLO level [1],

$$\mathcal{H}_{eff} = -\frac{G_F}{\sqrt{2}}\frac{\alpha}{2\pi\sin^2\theta_W}\left[V_{cs}^*V_{cd}Y_{NL} + V_{ts}^*V_{td}Y(x_t)\right] \times(\bar{s}d)_{V-A}(\bar{\mu}\mu)_{V-A} + h.c. \quad (46)$$

where the functions $Y(x_t)$ and Y_{NL} have been given in (17,19).

Using the effective Hamiltonian (46) and relating $< 0|(\bar{s}d)_{V-A}|K_L >$ to $Br(K^+ \to \mu^+\nu)$ one finds [37,2]

$$Br(K_L \to \mu^+\mu^-)_{SD} = \kappa_\mu \cdot \left[\frac{Re\lambda_c}{\lambda}P_0(Y)^{SM} + \frac{Re\lambda_t}{\lambda^5}Y(x_t)\right]^2 \quad (47)$$

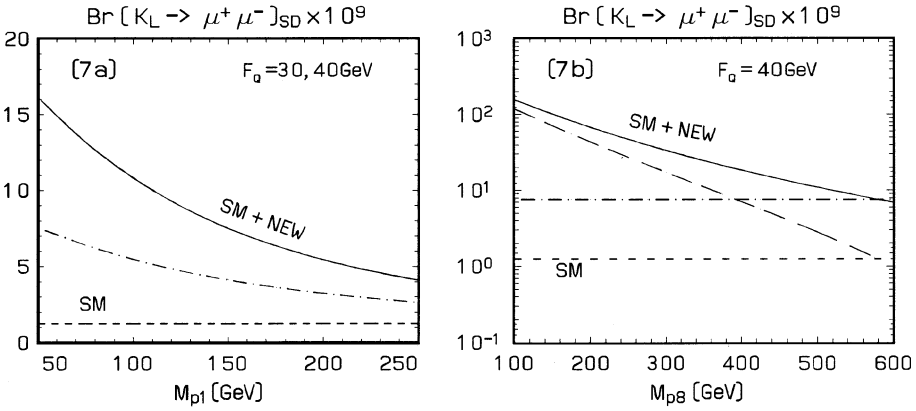

Fig. 7. a, **b** are the plots of the branching ratio $Br(K_L \to \mu^+\mu^-)_{SD}$ vs the mass m_{p1} and m_{p8} respectively. For more details see the text

with $\kappa_\mu = 1.68 \times 10^{-9}$[1].

Within the SM, using the input parameters of (27), one finds

$$Br(K_L \to \mu^+\mu^-)_{SD} = 1.25 \times 10^{-9} \tag{48}$$

which is consistent with the result as given in [1]. When the long-distance part is also included[1] one finds,

$$Br(K_L \to \mu^+\mu^-)_{TH} = (6.81 \pm 0.32) \times 10^{-9} \tag{49}$$

which is basically consistent with the data [9],

$$Br(K_L \to \mu^+\mu^-) = (7.2 \pm 0.5) \times 10^{-9} \tag{50}$$

the error of the data will be reduced to about $\pm 1\%$ at BNL in the next years.

When the new contributions due to π_1 and π_8 are included, one finds

$$Br(K_L \to \mu^+\mu^-)_{SD} = \kappa_\mu \cdot \left[\frac{Re\lambda_c}{\lambda} P_0(Y) + \frac{Re\lambda_t}{\lambda^5} Y(x_t, y_t, z_t)\right]^2 \tag{51}$$

where $\kappa_\mu = 1.68 \times 10^{-9}$[1]. By using the input parameters of (27) and assuming $F_Q = 40\,\text{GeV}$, $50\,\text{GeV} \le m_{p1} \le 400\,\text{GeV}$ and $100\,\text{GeV} \le m_{p8} \le 600\,\text{GeV}$, one has

$$1.71 \times 10^{-9} \le Br(K_L \to \mu^+\mu^-)_{SD} \le 7.55 \times 10^{-9} \tag{52}$$

if only the π_1's contribution is included, and

$$0.99 \times 10^{-9} \le Br(K_L \to \mu^+\mu^-)_{SD} \le 1.19 \times 10^{-7} \tag{53}$$

if only the π_8's contribution is included, and

$$1.42 \times 10^{-9} \le Br(K_L \to \mu^+\mu^-)_{SD} \le 1.57 \times 10^{-7} \tag{54}$$

if the π_1's and π_8's contribution are all included. For the typical values of $m_{p1} = 200\,\text{GeV}$ and $m_{p8} = 300\,\text{GeV}$, one finds $Br(K_L \to \mu^+\mu^-)_{SD}(\pi_1) = 3.24 \times 10^{-9}$, $Br(K_L \to \mu^+\mu^-)_{SD}(\pi_8) = 1.72 \times 10^{-8}$ and $Br(K_L \to \mu^+\mu^-)_{SD}(All) = 2.34 \times 10^{-8}$.

Figure 7a shows the m_{p1} dependence of the branching ratio $Br(K_L \to \mu^+\mu^-)_{SD}$ when only the extra contribution from π_1 is included, where the solid (dot-dashed) curve corresponds to the theoretical predictions for $Br(K_L \to \mu^+\mu^-)_{SD}$ with the inclusion of the contribution due to π_1 for $F_Q = 30, 40\,\text{GeV}$ respectively. Figure 7b shows the m_{p8} dependence of the branching ratio $Br(K_L \to \mu^+\mu^-)_{SD}$ when the contributions from both π_1 and π_8 are considered. The short-dashed line shows the SM prediction $Br(K_L \to \mu^+\mu^-)_{SD} = 1.25 \times 10^{-9}$, while the dot-dashed line shows the branching ratio $Br(K_L \to \mu^+\mu^-)_{SD} = 7.55 \times 10^{-9}$ for $m_{p1} = 50\,\text{GeV}$. The long-dashed curve shows the branching ratio when only the extra contribution from the π_8 is included. The solid curve corresponds to the branching ratio when all new contributions are taken into account.

The situation for the decay $K_L \to \mu^+\mu^-$ is rather subtle because of the involvement of the long-distance part. Firstly, the experimental data is accurate and basically consistent with the current theoretical predictions for the decay $K_L \to \mu^+\mu^-$ in the SM. Secondly, the calculation for the short-distance part is rather reliable. And finally the size of the new physics contributions strongly depend on the masses of new particles as shown in Fig. 7. It seems that this decay mode should be very helpful for us to test the SM and to probe the effects of the new physics beyond the SM, or at least to put some limits on the masses of new particles. But it is very difficult to calculate the long-distance contribution reliably, the current result is only an estimation based on some general assumptions and inevitably has large uncertainty. This fact makes it difficult to get a reliable theoretical prediction for the decay $K_L \to \mu^+\mu^-$ at present.

As an estimation, we at first conservatively assume that the uncertainty of the current theoretical prediction for the decay $K_L \to \mu^+\mu^-$ is two times larger than that given in (49), i.e.,

$$Br(K_L \to \mu^+\mu^-)_{TH} = (6.81 \pm 0.96) \times 10^{-9} \tag{55}$$

and to see if we can find any bounds on the masses of the π_1 and π_8 by comparing the theoretical prediction (55) with the experimental data (50).

Figure 8a is the plot of the branching ratio $Br(K_L \to \mu^+\mu^-)$ as a function of the mass m_{p1} assuming $F_Q = 40\,\text{GeV}$. The three curves are the theoretical predictions with the inclusion of the new contribution from π_1 only, and the horizontal band shows the experimental data (50).

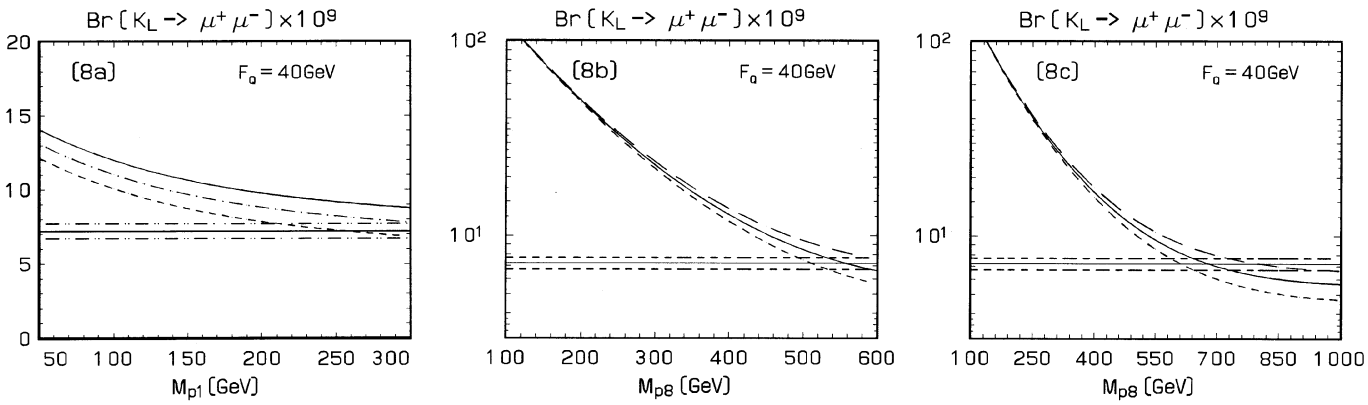

Fig. 8. a, **b** show the lower bounds on the mass of the π_1 and π_8 assuming $F_Q = 40\,\text{GeV}$. The horizontal band corresponds to the current experimental data, the three curves are the theoretical predictions when we use the enlarged uncertainty of $Br(K_L \to \mu^+\mu^-)_{TH}$. The Fig. 8c shows the lower bounds on the mass of the π_8 if we use ± 0.32 instead of the enlarged ± 0.96 as the uncertainty of the theoretical prediction. One can read the lower bounds on the masses of the π_1 and π_8

One can read the lower bound on m_{p1} from the Fig. 8a:

$$m_{p1} \geq 210\,\text{GeV} \tag{56}$$

when we neglect the contributions to the rare decay $K_L \to \mu^+\mu^-$ from the π_8. For $F_Q = 30\,\text{GeV}$, the corresponding lower bound is $m_{p1} \geq 313\,\text{GeV}$. If we treat the theoretical prediction $Br(K_L \to \mu^+\mu^-)_{TH} = 6.81 \pm 0.32$ as a reliable one the corresponding lower mass bounds are $m_{p1} \geq 262$, or, 355 GeV for $F_Q = 40, 30\,\text{GeV}$ respectively. For $F_Q = 40\,\text{GeV}$ and $m_{p8} \leq 490\,\text{GeV}$ the whole parameter space for m_{p1} is excluded completely.

From Fig. 8b one can read the constraints on the m_{p8}. The horizontal band corresponds to the data, while the three curves are the theoretical predictions with the inclusion of the contributions from the π_8 only. By comparing the theoretical predictions (with the enlarged theoretical uncertainty ± 0.96) with the data one finds the lower bounds on m_{p8}:

$$m_{p8} \geq \begin{cases} 490\,\text{GeV for} & F_Q = 40 \quad \text{GeV} \\ 527\,\text{GeV for} & F_Q = 30 \quad \text{GeV} \end{cases} \tag{57}$$

If we take the theoretical uncertainty ± 0.32 as a reliable one, the above lower bounds on m_{p8} will be increased by about 20 GeV.

Figure 8c is the plot of the branching ratio $Br(K_L \to \mu^+\mu^-)$ as a function of the mass m_{p8} assuming $m_{p1} = 210\,\text{GeV}$ and $F_Q = 40\,\text{GeV}$. The three curves are the theoretical predictions with the inclusion of the contributions from the π_1 and π_8. By comparing the theoretical predictions (with the enlarged theoretical uncertainty ± 0.96) with the data one finds the lower bounds on m_{p8}:

$$m_{p8} \geq \begin{cases} 580\,\text{GeV for} & F_Q = 40 \quad \text{GeV} \\ 630\,\text{GeV for} & F_Q = 30 \quad \text{GeV} \end{cases} \tag{58}$$

If we take the theoretical uncertainty ± 0.32 as a reliable one, the above lower bounds on m_{p8} will be increased by about 20 GeV.

One can see from (56, 57, 58) the lower bounds on m_{p1} and m_{p8} are rather stringent. Although the theoretical uncertainty for the long-distance part of the branching ratio $Br(K_L \to \mu^+\mu^-)$ is still large, but the current experimental data leads to a meaningful and stringent constraints on the mass spectrum of unit-charged technipions and consequently on the multiscale walking technicolor model itself.

In [12], the authors constructed a specific multiscale walking technicolor model and calculated the dijet and technipion production rates at the hadron colliders by using two sets of input mass parameters (4, 5). But the assumed mass ranges of the π_1 and π_8 are clearly excluded by the constraints from the rare K-decay process $K_L \to \mu^+\mu^-$ as given in (56, 57, 58). Although the detailed study about the specific model constructed in [12] is clearly beyond the scope of this paper, but the assumed mass spectrums for unit-charged technipions as given in [12] are excluded by the data, according to our calculations.

6 Conclusion and discussions

In this paper we calculate the Z^0-penguin contributions to the rare FCNC K-decays $K^+ \to \pi^+\nu\overline{\nu}$, $K_L \to \pi^0\nu\overline{\nu}$ and $K_L \to \mu^+\mu^-$ from the unit-charged technipions π_1 and π_8 appeared in the MWTCM [12].

We firstly evaluate the new Z^0-penguin diagrams induced by the π_1 and π_8, and extract the finite functions $C_0^{New}(y_j)$, $C_0^{New}(z_j)$, $C_{NL}(\pi_1)$ and $C_{NL}(\pi_8)$ which govern the new contributions to the decay in question and plays the same rule as the functions $C_0(x_i)$ and C_{NL} in [1] for the study of rare K-decays. The color-octet π_8 does not contribute to the decay through the box-diagrams, while the tiny box-diagram contributions from π_1 can be neglected safely. The charged technipions contribute to the branching ratios of the rare K-decays through the functions C_0^{New} and C_{NL}^{New} by a proper linear combination with their Standard Model counterparts $C_0(x_t)$ and C_{NL}.

The size of the new contributions generally depends on the value of the technipion decay constant F_Q and the mass spectrum of the charged technipions, and the color-octet π_8 dominant in a large part of the parameter space.

At the level of the corresponding branching ratios, the maximum enhancement due to π_1 is about one order of magnitude. While the maximum enhancement due to π_8 can be as large as two orders. So strong enhancements to the relevant branching ratios of $Br(K^+ \to \pi^+\nu\bar{\nu})$ and $Br(K_L \to \mu^+\mu^-)$ make it possible to put some constraints on the mass spectrum of charged technipions by comparing the theoretical predictions with the experimental data available.

For the decay $K^+ \to \pi^+\nu\overline{\nu}$, as illustrated in Figs. 5a–c, there is no independent constraint on m_{p1} at present, but further refinement of the data may put some constraints on m_{p1} in the near future. For the color-octet technipion π_8, the typical constraints are $m_{p8} \geq 228\,\mathrm{GeV}$ assuming $F_Q = 40\,\mathrm{GeV}$ and $m_{p1} = 200\,\mathrm{GeV}$, and $m_{p8} \geq 341\,\mathrm{GeV}$ assuming $F_Q = 30\,\mathrm{GeV}$ and $m_{p1} = 200\,\mathrm{GeV}$.

For the decay $K_L \to \pi^0\nu\overline{\nu}$, as shown in Figs. 6a,b, no constraint on both m_{p1} and m_{p8} can be derived now because of the low sensitivity of the available data.

For the decay $K_L \to \mu^+\mu^-$, the situation is rather subtle because of the involvement of the long-distance part. Our attempt to constrain the new physics models is hampered to some degree by the large uncertainty of the long-distance piece of the branching ratio $Br(K_L \to \mu^+\mu^-)$. Fortunately, thanks to the accurate experimental data published by the E787 collaboration, rather strong constraints have been obtained even if we use the enlarged uncertainty of $Br(K_L \to \mu^+\mu^-)_{TH}$.

For the color-singlet π_1, the lower mass bound is $m_{p1} \geq 210\,\mathrm{GeV}$ if we neglect the new contribution to the decay $(K_L \to \mu^+\mu^-)_{SD}$ from the color-octet π_8. For $F_Q = 30\,\mathrm{GeV}$, the corresponding lower bound is $m_{p1} \geq 313\,\mathrm{GeV}$. If we treat the theoretical prediction $Br(K_L \to \mu^+\mu^-)_{TH} = 6.81 \pm 0.32$ as a reliable one the corresponding lower mass bounds are $m_{p1} \geq 262$, or, 355 GeV for $F_Q = 40$, 30 GeV respectively. For $F_Q = 40\,\mathrm{GeV}$ and $m_{p8} \leq 490\,\mathrm{GeV}$, the whole assumed parameter space for π_1, $50\,\mathrm{GeV} \leq m_{p1} \leq 400\,\mathrm{GeV}$, is excluded completely by the data.

For color-octet technipion π_8, the lower bounds on m_{p8} are much stronger than that on m_{p1}. If we neglect the π_1's contributions to the branching ratio $Br(K_L \to \mu^+\mu^-)_{SD}$ and use the enlarged theoretical uncertainty $\delta Br(K_L \to \mu^+\mu^-)_{TH} = 0.96$, the lower bounds on m_{p8} are $m_{p8} \geq 490\,\mathrm{GeV}$ (527 GeV) for $F_Q = 40\,\mathrm{GeV}$ (30 GeV). The above lower bounds on m_{p8} will be increased by about 20 GeV, If we take the theoretical uncertainty ± 0.32 as a reliable one.

If we take into account the contributions due to the π_1 (assuming $m_{p1} = 210\,\mathrm{GeV}$) and use the enlarged theoretical uncertainty $\delta Br(K_L \to \mu^+\mu^-)_{TH} = 0.96$, the lower bounds on m_{p8} are $m_{p8} \geq 580\,\mathrm{GeV}$ (630 GeV) for $F_Q = 40\,\mathrm{GeV}$ (30 GeV). The above lower bounds on m_{p8} will be increased again by about 20 GeV, If we take the theoretical uncertainty ± 0.32 as a reliable one.

For intrinsic and technical reasons, it is very difficult to calculate the strong ETC and walking technicolor interactions reliably. But one can use the currently known knowledge to make primary estimations about the possible contributions to various physical processes from the new particles appeared in the MWTCM, and in turn to test the model itself or constrain the parameter space of the model. In [38], the authors examined the corrections to the branching ratio $R_b = \Gamma(Z \to b\bar{b})/\Gamma(Z \to hadron)$ due to the exchanges of the ETC gauge bosons and found that the new contribution is too large to be consistent with the LEP data in most of the parameter space in the MWTCM[38]. In [39], the authors estimated the corrections to the rare decay $b \to s\gamma$ in the MWTCM, and found that the whole range of $m_{p8} \leq 600\,\mathrm{GeV}$ is excluded by the CLEO data of $Br(B \to X_s\gamma) = (2.32 \pm 0.57 \pm 0.35) \times 10^{-4}$[39]. In this paper, we studied the new contributions to the rare K-decays from the unit-charged technipions in the framework of the MWTCM. The resulted constraints on the m_{p1} and m_{p8} from the data (50) are rather stringent. The main cause which leads to the above constraints is the smallness of the F_Q (which is clearly a basic feature of the MWTCM). If we treat above results seriously, one conclusion is inevitable: the smallness of F_Q is disfavored by the $Br(K_L \to \mu^+\mu^-)$ and R_b data, and the assumed mass parameter space for the π_1 and π_8 as given in [12] is excluded by the data (50) as well as the CLEO data for rare decay $b \to s\gamma$, and therefore the multiscale walking technicolor model itself as constructed in [12] is strongly disfavored by the data. One way out is to modify the multiscale walking technicolor model by introducing the Topcolor interaction [40] into the model [41].

Acknowledgement. Z. Xiao would like to thank R.G. Roberts and all friends in the Theory Group at the Rutherford-Appleton Laboratory for their hospitality and support. This work was partly done during my stay at RAL as a visitor. This work is supported by the National Science Foundation of China and by the Sino-British Friendship Scholarship Scheme.

Appendix A

In this Appendix, we present the explicit expressions for the functions $C_0(x_t)$, $B_0(x_t)$, $X_1(x_t)$, $Y_1(x_t)$, C_{NL}, $B_{NL}^{1/2}$, $B_{NL}^{-1/2}$, $C_{NL}(\pi_1)$ and $C_{NL}(\pi_8)$. One can also find the expressions for the first seven functions in [2].

The functions of $C_0(x_t)$ and $B_0(x_t)$ govern the leading top quark contributions through the Z^0-penguin and W-box diagrams in the SM, while the functions $X_1(x_t)$ and $Y_1(x_t)$ describe the NLO QCD corrections,

$$B_0(x_t) = \frac{1}{4}\left[\frac{x_t}{1-x_t} + \frac{x_t \ln[x_t]}{(x_t-1)^2}\right] \tag{59}$$

$$C_0(x_t) = \frac{x_t}{8}\left[\frac{x_t-6}{x_t-1} + \frac{3x_t+2}{(x_t-1)^2}\ln[x_t]\right] \tag{60}$$

$$\begin{aligned} X_1(x_t) = &-\frac{23x_t + 5x_t^2 - 4x_t^3}{3(1-x_t)^2} \\ &+\frac{x_t - 11x_t^2 + x_t^3 + x_t^4}{(1-x_t)^3}\ln[x_t] \\ &+\frac{8x_t + 4x_t^2 + x_t^3 - x_t^4}{2(1-x_t)^3}\ln^2[x_t] \end{aligned}$$

$$
\begin{aligned}
&-\frac{4x_t - x_t^3}{(1-x_t)^2} L_2(1-x_t) \\
&+8x_t \frac{\partial X_0(x_t)}{\partial x_t} \ln[x_\mu] \qquad (61)\\
Y_1(x_t) = &-\frac{4x_t + 16x_t^2 + 4x_t^3}{3(1-x_t)^2} \\
&-\frac{4x_t - 10x_t^2 - x_t^3 - x_t^4}{(1-x_t)^3} \ln[x_t] \\
&+\frac{2x_t - 4x_t^2 + x_t^3 - x_t^4}{2(1-x_t)^3} \ln^2[x_t] \\
&-\frac{2x_t + x_t^3}{(1-x_t)^2} L_2(1-x_t) \\
&+8x_t \frac{\partial Y_0(x_t)}{\partial x_t} \ln[x_\mu] \qquad (62)
\end{aligned}
$$

where $x_t = m_t^2/m_W^2$, $x_\mu = \mu^2/M_W^2$ with $\mu = \mathcal{O}(m_t)$ and

$$
L_2(1-x_t) = \int_1^{x_t} dy \, \frac{ln[y]}{1-y}. \qquad (63)
$$

For the charm sector, the C_{NL} is the Z^0-penguin part and the $B_{NL}^{1/2}$ ($B_{NL}^{-1/2}$) is the box contribution, relevant for the case of final state leptons with $T_3 = 1/2$ ($T_3 = -1/2$):

$$
\begin{aligned}
C_{NL} = &\frac{x(m)}{32} K_c^{24/25} \left[\left(\frac{48}{7} K_+ + \frac{24}{11} K_- - \frac{696}{77} K_{k33} \right) \right. \\
&\times \left(\frac{4\pi}{\alpha_s(\mu)} + \frac{15212}{1875}(1 - K_c^{-1}) \right) \\
&+ \left(1 - \ln \frac{\mu^2}{m^2} \right) (16K_+ - 8K_-) - \frac{1176244}{13125} K_+ \\
&-\frac{2302}{6875} K_- + \frac{3529184}{48125} K_{33} \qquad (64)\\
&\left. + K \left(\frac{56248}{4375} K_+ - \frac{81448}{6875} K_- + \frac{4563698}{144375} K_{33} \right) \right]
\end{aligned}
$$

where

$$
\begin{aligned}
&K = \frac{\alpha_s(M_W)}{\alpha_s(\mu)}, \quad K_c = \frac{\alpha_s(\mu)}{\alpha_s(m)}, \quad K_+ = K^{6/25}, \\
&K_- = K^{-12/25}, \quad K_{33} = K^{-1/25} \qquad (65)
\end{aligned}
$$

and

$$
\begin{aligned}
B_{NL}^{1/2} = &\frac{x(m)}{4} K_c^{24/25} \left[3(1-K_2) \left(\frac{4\pi}{\alpha_s(\mu)} \right. \right. \\
&\left. + \frac{15212}{1875}(1 - K_c^{-1}) \right) - \ln \frac{\mu^2}{m^2} \\
&\left. - \frac{r \ln r}{1-r} - \frac{305}{12} + \frac{15212}{625} K_2 + \frac{15581}{7500} K \, K_2 \right] \qquad (66)\\
B_{NL}^{-1/2} = &\frac{x(m)}{4} K_c^{24/25} \left[3(1-K_2) \left(\frac{4\pi}{\alpha_s(\mu)} \right. \right. \\
&\left. + \frac{15212}{1875}(1 - K_c^{-1}) \right) - \ln \frac{\mu^2}{m^2} - \frac{329}{12} \\
&\left. + \frac{15212}{625} K_2 + \frac{30581}{7500} K \, K_2 \right] \qquad (67)
\end{aligned}
$$

here $K_2 = K_{33}$, $m = m_c$, $\mu = \mathcal{O}(m_c)$, $x(m) = m_c^2/M_W^2$, $r = m_l^2/m_c^2(\mu)$ and m_l is the lepton mass.

For the charm sector, the functions of $C_{NL}(\pi_1)$ and $C_{NL}(\pi_8)$ describe the contributions from the π_1 and π_8,

$$
\begin{aligned}
C_{NL}(\pi_1) = &a_1 \, K_c^{24/25} \left[\left(\frac{48}{7} K_+^{\pi_1} + \frac{24}{11} K_-^{\pi_1} - \frac{696}{77} K_{k33}^{\pi_1} \right) \right. \\
&\times \left(\frac{4\pi}{\alpha_s(\mu)} + \frac{15212}{1875}(1 - K_c^{-1}) \right) \\
&+ \left(1 - \ln \frac{\mu^2}{m^2} \right) (16K_+^{\pi_1} - 8K_-^{\pi_1}) - \frac{1176244}{13125} K_+^{\pi_1} \\
&-\frac{2302}{6875} K_-^{\pi_1} + \frac{3529184}{48125} K_{33}^{\pi_1} \qquad (68)\\
&\left. + K_{\pi_1} \left(\frac{56248}{4375} K_+^{\pi_1} - \frac{81448}{6875} K_-^{\pi_1} + \frac{4563698}{144375} K_{33}^{\pi_1} \right) \right]
\end{aligned}
$$

with

$$
\begin{aligned}
&a_1 = \frac{m_c^2}{768\sqrt{2} F_Q^2 G_F M_W^2}, \\
&K_{\pi_1} = \frac{\alpha_s(m_{p1})}{\alpha_s(\mu)}, \quad K_c = \frac{\alpha_s(\mu)}{\alpha_s(m)}, \\
&K_+^{\pi_1} = (K_{\pi_1})^{6/25}, \quad K_-^{\pi_1} = (K_{\pi_1})^{-12/25}, \\
&K_{33}^{\pi_1} = (K_{\pi_1})^{-1/25} \qquad (69)
\end{aligned}
$$

and

$$
\begin{aligned}
C_{NL}(\pi_8) = &a_8 \, K_c^{24/25} \left[\left(\frac{48}{7} K_+^{\pi_8} + \frac{24}{11} K_-^{\pi_8} - \frac{696}{77} K_{k33}^{\pi_8} \right) \right. \\
&\times \left(\frac{4\pi}{\alpha_s(\mu)} + \frac{15212}{1875}(1 - K_c^{-1}) \right) \\
&+ \left(1 - \ln \frac{\mu^2}{m^2} \right) (16K_+^{\pi_8} - 8K_-^{\pi_8}) \\
&-\frac{1176244}{13125} K_+^{\pi_8} - \frac{2302}{6875} K_-^{\pi_8} + \frac{3529184}{48125} K_{33}^{\pi_8} \qquad (70)\\
&\left. + K_{\pi_8} \left(\frac{56248}{4375} K_+^{\pi_8} - \frac{81448}{6875} K_-^{\pi_8} + \frac{4563698}{144375} K_{33}^{\pi_8} \right) \right]
\end{aligned}
$$

with

$$
\begin{aligned}
&a_8 = \frac{m_c^2}{96\sqrt{2} F_Q^2 G_F M_W^2}, \\
&K_{\pi_8} = \frac{\alpha_s(m_{p8})}{\alpha_s(\mu)}, \quad K_c = \frac{\alpha_s(\mu)}{\alpha_s(m)}, \\
&K_+^{\pi_8} = (K_{\pi_8})^{6/25}, \quad K_-^{\pi_8} = (K_{\pi_8})^{-12/25}, \\
&K_{33}^{\pi_8} = (K_{\pi_8})^{-1/25}. \qquad (71)
\end{aligned}
$$

References

1. A.J. Buras, R. Fleischer, hep-ph/9704376, to appear in Heavy Flavor II, eds. A.J. Buras, M. Lindner, World Scientific Publishing Co. Singapore
2. G. Buchalla, A.J. Buras, M.E. Lautenbacher, Rev. Mod. Phys. **68**, 1125 (1996)

3. J.O. Eeg, K. Kumericki, I. Picek, hep-ph/9605337, and reference therein
4. S. Weinberg, Phys. Rev. D **13**, 974 (1976); **19**, 1277 (1979); L. Susskind, ibid, **20**, 2619 (1979)
5. S. Dimopoulos, L. Susskind, Nucl. Phys. B **155**, 237 (1979); E. Eichten, K. Lane, Phys. Lett. **90B**, 125 (1980)
6. B. Holdom, Phys. Rev. D **24**, 1441 (1981); Phys. Lett. **150B**, 301 (1985); T. Appelquist, D. Karabali, L.C.R. Wijewardhana, Phys. Rev. Lett. **57**, 957 (1986)
7. E. Farhi, L. Susskind, Phys. Rev. D **20**, 3404 (1979)
8. M. Peskin, T. Takeuki, Phys. Rev. Lett **65**, 2967 (1990); M. Peskin, T. Takeuki, Phys. Rev. D **44**, 381 (1992)
9. Particle Data Group, C. Caso et al., Eur. Phys. J. C **3**, 1 (1998)
10. K. Lane, presented at the 28th International Conference on High Energy Physics (ICHEP 96), Warsaw (July 1996), ICHEP 96:307–318
11. M. Luty, R. Sundrum, Phys. Rev. Lett. **70**, 529 (1993); R. Sundrum, S. Hsu, Nucl. Phys. B **391**, 127 (1993); R. Sundrum, Nucl. Phys. B **395**, 60 (1993); T. Appelquist, J. Terning, Phys. Lett. **315B**, 139 (1993)
12. K. Lane, E. Eichten, Phys. Lett. **222B**, 274 (1989); K. Lane, M.V. Ramana, Phys. Rev. D **44**, 2678 (1991)
13. E. Eichten, K. Lane, Phys. Lett. **327B**, 129 (1994)
14. G. Buchalla, A.J. Buras, M.K. Harlander, Nucl. Phys. B **349**, 1 (1991)
15. Z.J. Xiao et al., The rare K-decays and the Z^0-penguin contributions from the charged technipions, HNU-preprint-TH/9809, April 1998 (unpublished)
16. I.I. Bigi, F. Gabbiani, Nucl. Phys. B **367**, 3 (1991)
17. M. Misiak, S. Pokorski, J. Rosiek, hep-ph/9703442, to appear in "Heavy Flavor II", eds. A.J. Buras, M. Lindner, World Scientific Publishing Co. Singapore
18. G. Burdman, Constraints on strong dynamics from rare B and K decays, MADPH-98-1039, hep-ph/9802232
19. C. Lü, Z. Xiao, Phys. Rev. D **53**, 2529 (1996);
20. E. Eichten, I. Hinchliffe, K. Lane, C. Quigg, Rev. Mod. Phys. **56**, 759 (1984); Phys. Rev. D **34**, 1547 (1986)
21. J. Womersley, Fermilab-Conf-96/431, hep-ph/9612281
22. E. Eichten, K. Lane, Phys. Rev. D **56**, 579 (1997);
23. S. Glashaw, S. Weinberg, Phys. Rev. D **15**, 1958 (1977)
24. J.P. Martin, LYCEN-9644, in Proceedings of the 28th IHEP, Warsaw, Poland, 25–31 July 1996, edited by Z. Ajduk, A.K. Wroblewski (World Scientific, Singapore,1997)
25. S. Chadha, M. Peskin, Nucl. Phys. B **185**, 61 (1981); B **187**, 541 (1981)
26. J. Ellis et al., Nucl. Phys. B **182**, 505 (1981)
27. T.P. Cheng, L.F. Li, Gauge theory of elementary particle physics, Clarendon Press, Oxford, 1984
28. T. Inami, C.S. Lim, Prog. Theor. Phys. **65**, 297 (1981)
29. P. Cho, B. Greistein, Nucl. Phys. B **365**, 365 (1991)
30. G. Buchalla, A.J. Buras, Nucl. Phys. B **400**, 225 (1993)
31. E787 Collaboration, S. Adler et al., Phys. Rev. Lett. **79**, 2204 (1997)
32. P. Cooper, M. Crisler, B. Tschirhart, J. Ritchie (CKM collaboration), EOI for measuring $Br(K^+ \to \pi^+ \nu\bar{\nu})$ at the Main Injector, Fermilab EOI 14, 1996
33. L. Littenberg, J. Sandweiss, eds., AGS2000, Experiments for the 21st Century, BNL 52512
34. L. Littenberg, Phys. Rev. D **39**, 3322 (1989)
35. M. Weaver et al., Phys. Rev. Lett. **72**, 3758 (1994)
36. K. Arisaka et al., KAMI conceptual design report, FNAL, June 1991
37. G. Buchalla, A.J. Buras, Nucl. Phys. B **412**, 106 (1994)
38. C.Y. Yue, Y.P. Kuang, G.R. Lu, J. Phys. G **23**, 163 (1997)
39. G.R. Lu, Y.G. Cao, Z.H. Xiong, C.Y. Yue, Z. Phys. C **74**, 355 (1997)
40. C.T. Hill, Phys. Lett. **345B**, 48391995); K. Lane, E. Eichten, *ibid*, **352**, 382 (1995)
41. Z.J. Xiao et al., in preparation